An ideal MHD δW stability analysis that bypasses the Newcomb equation

Cite as: Phys. Plasmas **27**, 022114 (2020); https://doi.org/10.1063/1.5109160
Submitted: 07 May 2019 . Accepted: 16 January 2020 . Published Online: 19 February 2020

Alexander S. Glasser, A. H. Glasser, Rory Conlin, and Egemen Kolemen

Physics of Plasmas ARTICLE scitation.org/journal/php

An ideal MHD δW stability analysis that bypasses the Newcomb equation

Cite as: Phys. Plasmas **27**, 022114 (2020); doi: 10.1063/1.5109160
Submitted: 7 May 2019 · Accepted: 16 January 2020 ·
Published Online: 19 February 2020

Alexander S. Glasser,[1] A. H. Glasser,[2] Rory Conlin,[3] and Egemen Kolemen[4,a)]

AFFILIATIONS

[1]Department of Astrophysical Sciences, Princeton University, Princeton, New Jersey 08540, USA
[2]Fusion Theory and Computation, Inc., Kingston, Washington 98346, USA
[3]Department of Mechanical and Aerospace Engineering, Princeton University, Princeton, New Jersey 08540, USA
[4]Princeton Plasma Physics Laboratory, Princeton, New Jersey 08543, USA

[a)]Author to whom correspondence should be addressed: ekolemen@princeton.edu

ABSTRACT

In the following work, we demonstrate the efficacy of a Riccati δW ideal MHD stability analysis that bypasses the numerically intractable integration of the Newcomb equation. By transforming the linear Newcomb equation into a quadratic Riccati equation, an accurate and equivalent δW analysis is performed that is shown to enjoy some numerical advantages. We demonstrate that the Riccati approach is better conditioned than its Newcomb counterpart at the magnetic axis, and we apply dynamical systems insights to examine its behavior at singular points. We further discuss the constraints involved in solving for the extremal admissible perturbations of a δW analysis.

I. INTRODUCTION

The ideal MHD energy principle,[1] as formulated in 1958 by Bernstein *et al.*,[2] states that a plasma equilibrium is stable if and only if $\delta W(\xi^*, \xi) \geq 0$ for all admissible perturbations ξ. Here, $\delta W(\xi^*, \xi)$ represents the change in potential energy away from equilibrium due to ξ, a plasma displacement. The set of admissible perturbations is generally defined to include any displacement ξ that everywhere satisfies $\delta W(\xi^*, \xi) < \infty$.

In 1960, this energy principle was applied to the cylindrical screw pinch by Newcomb,[3] who analyzed fixed-boundary perturbations (a fixed-boundary, or internal, perturbation ξ satisfies $\xi|_{r=1} = 0$ at the plasma edge). Newcomb derived an ordinary differential equation (ODE) satisfied by such perturbations and showed that its integration determined a stability criterion for the screw pinch. Newcomb's procedure was generalized in A. H. Glasser's DCON code,[4] which defined the stability criteria for fixed- and free-boundary perturbations in axisymmetric toroidal plasmas [a free-boundary (or external) perturbation occurs in a plasma surrounded by a vacuum region rather than a conducting wall and therefore allows $\xi|_{r=1} \neq 0$]. It was more recently pointed out in Ref. 5 that the δW analysis of DCON was equivalent to a Riccati problem, for which there exist well-established numerical methods in the control theory literature.

Riccati problems often arise in optimal control applications when a cost functional being optimized over time is quadratic in the system's state variables and control inputs.[6–8] Treating its radial coordinate as an effective time parameter, the perturbed energy functional $\delta W(\xi^*, \xi)$ has an analogous quadratic form, and its minimization can therefore be solved by a radial—rather than temporal—Riccati ODE.

Although Riccati ODEs are nonlinear, they can generally be reexpressed as linear ODEs by a coordinate transformation. This transformation is a common strategy[8–10] for solving Riccati problems and can be advantageous for applications that prioritize solution speed, as demonstrated in the parallelized MHD stability code STRIDE, of Refs. 5 and 11.

In especially large or stiff problems (a characterization often appropriate to a δW analysis), however, this linear approach can be impractical.[12] Perturbations of toroidal plasma equilibria are often challenging in just this way: They may require many Fourier modes to be accurately resolved, and the linear Newcomb equation exhibits stiff behavior at scales spanning many orders of magnitude. Such numerical problems can be exacerbated in the analysis of perturbations with high mode numbers or in equilibria whose perturbations couple across toroidal modes (as in stellarators).

In the present work, we therefore take the opposite approach: We sidestep the linear toroidal Newcomb equation by reexpressing it as a quadratic Riccati ODE; in short, we solve Eq. (29) of the present paper rather than Eq. (27). We numerically implement a Riccati δW analysis for toroidal plasmas and demonstrate its accuracy. In so doing, we

address questions that arise in the solution of the δW Riccati ODE, especially with respect to its singularities.

The remainder of this paper is organized as follows: In Sec. II, we summarize the Riccati formulation of the δW problem for the cylindrical screw pinch and emphasize its equivalence to Newcomb's procedure. In Sec. III, we analyze the asymptotic behavior of the cylindrical Riccati ODE at its singular points. In Sec. IV, we discuss the Riccati δW problem for an axisymmetric toroidal equilibrium, and we describe our solution methods for it.

In Sec. V, we benchmark the numerical results of our toroidal Riccati formulation against DCON's δW analysis, and we describe the numerical advantages of the Riccati approach. In particular, we show that the Riccati equation—while sacrificing the linearity and solution speed of the Newcomb equation—significantly moderates the stiff mode growth of the Newcomb system at the magnetic axis. Furthermore, unlike solutions to the Newcomb equation, Riccati solutions are found to be finite at rational surfaces. In Sec. VI, we discuss the constraints imposed by the admissibility criterion $\delta W(\xi^*, \xi) < \infty$ on the behavior of extremal perturbations. In Sec. VII, we summarize our results and conclude.

II. NEWCOMB'S SCREW PINCH STABILITY CRITERION IN THE RICCATI FORMULATION

To introduce the Riccati formulation of the δW problem, we first describe the cylindrical case in some detail. We begin with the Lagrangian for δW, the change in plasma potential energy in a cylindrical screw pinch[3] due to a perturbed mode $\xi(r)\exp[i(m\theta + kz)]$

$$\delta W = \int_0^1 L(r, \xi, \xi')\mathrm{d}r = \frac{1}{2}\int_0^1 \left[f(\xi')^2 + g\xi^2\right]\mathrm{d}r, \tag{1}$$

where $' \equiv d/dr$. [following Newcomb's familiar expression for $\mathrm{d}W$, Eq. (1) omits a surface contribution to the perturbed plasma potential energy (see Ref. 1, Eq. 11.89). We note that referring to a cost functional as a "Lagrangian" is standard nomenclature in control theory, although we emphasize that our cost function is integrated radially, rather than over time.] Letting $\mu(r)^2 \equiv m^2 + k^2r^2$, the functions $f(r)$ and $g(r)$ are defined as follows:

$$\begin{aligned} f(r) &= \frac{k^2r^3B_z(r)^2}{\mu(r)^2}\left(1 - \frac{m}{q(r)}\right)^2, \\ g(r) &= f(r)\left[\frac{2k^2}{\mu(r)^2}\frac{1 + \dfrac{m}{q(r)}}{1 - \dfrac{m}{q(r)}} + \frac{\mu(r)^2 - 1}{r^2}\right] + \frac{2k^2}{\mu(r)^2}r^2p'(r). \end{aligned} \tag{2}$$

Here, $q(r) \equiv -krB_z(r)/B_\theta(r)$ denotes the safety factor (with effective toroidal mode number $n = 1$ and $k \equiv n/R_0$), $\mathbf{B}(r)$ the magnetic field, and $p(r)$ the pressure profile. We observe that $f(r) \geq 0\ \forall\ r$.

In accordance with the energy principle, we seek to characterize plasma stability by searching for perturbations that minimize δW. However, the minimization of δW is in general complicated by the fact that variations of Eq. (1) may not be positive-definite. We recall the following results from the calculus of variations, regarding criteria for the optimality of any $\xi(r)$.[13–15]

1. (Necessary criterion) Any perturbation $\xi(r)$ that minimizes δW satisfies the Euler-Lagrange equation of δW (i.e., Newcomb's equation)

$$-(f\xi')' + g\xi = 0. \tag{3}$$

We observe that this cylindrical Newcomb equation has singularities where $f(r) = 0$—namely, at the magnetic axis ($r = 0$) and at rational surfaces r_s where the safety factor satisfies $q(r_s) = m$.

To state the second optimality criterion, we first define a *conjugate point*. Given a solution $\xi_0(r)$ of Eq. (3) on an interval $[a, b]$, which satisfies $\xi_0(a) = 0$ and is not identically zero, a point $r_0 \in (a, b]$ is *conjugate* to a if $\xi_0(r_0) = 0$. With this definition, we note:

2. (Sufficient criterion) An extremal $\xi(r)$ is a strict minimum of δW on the interval $[a, b]$ if $\partial^2L/\partial\xi'\partial\xi' > 0\ \forall\ r \in [a, b]$ and $(a, b]$ contains no points conjugate to a.

Newcomb's δW analysis generalizes these criteria to test for fixed-boundary mode stability in a screw pinch. In particular, although above the sufficient condition is restricted to intervals on which $\partial^2L/\partial\xi'\partial\xi' = f > 0$, Newcomb demonstrates that his procedure suffices as a test of stability for all admissible perturbations of a general equilibrium, including those with rational surfaces r_s, where $f(r_s) = 0$.

We summarize the Newcomb procedure as follows: (i) Suydam's criterion[16] (to be defined) is checked for interchange stability; (ii) assuming that Suydam's criterion is satisfied, Eq. (3) is integrated from the magnetic axis ($r = 0$) to the plasma edge ($r = 1$), with initial condition $\xi|_{r=0} = 0$; (iii) after each rational surface $0 < r_s < 1$—where the ODE is singular—ξ is re-initialized again with a "small" solution (to be defined) and integrated forward; (iv) if the resulting integrated solution has any conjugate points $r_0 \notin \{0, r_s\}$—that is, if ξ has a zero-crossing for any $r_0 \in [0, 1]$ such that $f(r_0) \neq 0$—then, the plasma is unstable to fixed-boundary modes; otherwise, it is stable to such modes.

The conjugate points of Newcomb's analysis arise when δW fails to be positive-definite. Roughly speaking, therefore, Newcomb demonstrates that whenever δW is not positive-definite, an admissible perturbation can be constructed satisfying $\delta W < 0$.

We now reexpress this Newcomb procedure in its equivalent Riccati formulation. The Riccati ODE commonly arises in control theory as the solution of a linear quadratic regulator (LQR) problem for a quadratic cost function integrated over time (see, e.g., Ref. 7): $\int[Qx^2 + Ru^2]\mathrm{d}t$, where $\dot{x} = Ax + Bu$. In the present problem, the same structure is found in the quadratic Lagrangian of Eq. (1), where $(x, u) \equiv (\xi, \xi')$, $\dot{x} = u$, and r is an effective time parameter.

Following the LQR prescription, we define the Riccati variable P as a linear map $\lambda = Px$ from a perturbation ($x \equiv \xi$) to its conjugate momentum, $\lambda \equiv \partial L/\partial\xi' = f\xi'$, namely,

$$P \equiv \frac{\lambda}{x} = \frac{f\xi'}{\xi}. \tag{4}$$

Using P to eliminate ξ' from Eq. (3), we find

$$P' = g - \frac{P^2}{f}. \tag{5}$$

Equation (5) is the cylindrical Riccati ODE, which provides an alternative to solving Newcomb's equation in a δW analysis.

We perform steps (ii)–(iv) of Newcomb's δW procedure in the Riccati formulation as follows: $P(0)$ is initialized according to Eq. (4) to reflect Newcomb's initial conditions $[\xi;\ \xi'](0)$. We note that the Riccati ODE shares the same singular points—r such that $f(r) = 0$—as its Newcomb counterpart, and we similarly reinitialize $P(r_s)$ to the small solution (to be defined in Sec. III) at each rational surface. We further note that the conjugate points of Newcomb's procedure—r_0 such that $\xi(r_0) = 0$ and $f(r_0) \neq 0$—correspond to infinites of P, namely, points where $\lim_{\epsilon\to 0} P(r_0 \pm \epsilon) = \pm\infty$. Therefore, in the Riccati approach, instead of integrating Eq. (3) and monitoring for conjugate points where $\xi(r_0) = 0$ we equivalently integrate Eq. (5) and monitor for points r_0, where

$$D_C(r_0) \equiv \frac{1}{P(r_0)} = 0. \tag{6}$$

As in Newcomb's analysis, this condition indicates a plasma instability to fixed-boundary perturbations. (A toroidal analog of this *critical determinant* D_C—which we shall revisit in Sec. IV—was already derived in Ref. 4.) We have thus reconstructed the cylindrical Newcomb procedure in the Riccati formalism.

Although it is a mathematically equivalent formulation, the Riccati equation characterizes the equilibrium stability more directly than its Newcomb counterpart. This can be seen by defining $S(r) \equiv \frac{1}{2}\xi P \xi$. Conditional on P satisfying Eq. (5), we note

$$\frac{dS}{dr} = \xi\xi' P + \frac{1}{2}\xi^2 P' = \frac{1}{2}\left[f(\xi')^2 + g\xi^2\right]. \tag{7}$$

Comparing this expression to Eq. (1) and integrating, we get

$$S(r) \equiv \frac{1}{2}\xi(r)P(r)\xi(r) = \int_0^r L(\tilde{r}, \xi, \xi')\mathrm{d}\tilde{r}, \tag{8}$$

where we have set $S(0) = 0$. The Riccati variable $P(r)$ is therefore a bilinear form that maps a localized perturbation $\xi(r)$ to its associated cumulative extremal energetic cost $S(r)$ over the plasma subinterval $[0, r]$. It effectively calculates the energetic cost of an extremal perturbation ξ that takes the value $\xi(r)$ at r and satisfies $0 = S(0) = \frac{1}{2} f \xi \xi'|_{r=0}$. For this reason, P is referred to as the *plasma response*. [We note that, whereas the function $S(r)$ appears serendipitously chosen above, it may also be systematically derived as Hamilton's principal function in a Hamilton–Jacobi analysis, as shown in Ref. 5.]

It is therefore intuitive that a negative infinity in the plasma response $P(r_0)$—at a surface r_0 where Eq. (6) is satisfied—indicates a plasma unstable to internal modes. After all, $P(r_{\epsilon^-})$ grows unboundedly negative as $r_{\epsilon^-} \equiv r_0 - \epsilon$ approaches r_0, such that for $\epsilon > 0$ small enough, no internal mode with a finite plasma response can be constructed on $[r_{\epsilon^-}, 1]$ to sufficiently offset the associated negative energy, $S(r_{\epsilon^-}) \equiv \frac{1}{2}\xi^2 P(r_{\epsilon^-})$.

We note that a free-boundary stability analysis follows from Eq. (8) as well. In particular, assuming that an equilibrium satisfies Suydam's criterion and is stable to fixed-boundary modes—i.e., no conjugate points $D_C(r) = 0$ are found when integrating the Riccati ODE over $r \in [0, 1]$—then any solution ξ of Eq. (3) is not only extremal but minimizes δW. Accordingly, the Riccati solution $P(1)$ maps an edge perturbation to its minimal energy

$$S(1) = \frac{1}{2}\xi(1)P(1)\xi(1). \tag{9}$$

In particular, when Eq. (5) for $P(r)$ is integrated to the edge of an interchange- and fixed-boundary-stable equilibrium, then the $S(1)$ of Eq. (9) reflects the minimum cumulative energy consistent with an edge perturbation $\xi(1)$. $P(1)$ correspondingly determines the bulk plasma's energetic response to free-boundary modes. We denote this response as $W_P \equiv P(1)$.

To define a stability criterion for a free-boundary perturbation, we make a complete accounting of its associated energy. In particular, we must include a surface plasma energy that was omitted from Eq. (1), as well as the (always-stabilizing) energetic response of the surrounding magnetized vacuum. We denote these additional contributions to the perturbed energy by $\frac{1}{2} W_{\mathrm{edge}} \xi(1)^2$, where $W_{\mathrm{edge}} \equiv W_S + W_V$. The straightforward calculation of these surface and vacuum responses can be found in Eq. 11.98 of Ref. 1 and is performed independently of W_P.

Therefore, a plasma equilibrium is unstable to free-boundary modes if

$$W_P + W_{\mathrm{edge}} < 0. \tag{10}$$

We have thus found an alternative ODE—Eq. (5)—that can be integrated in lieu of the Newcomb equation for the δW analysis of the screw pinch. Newcomb's zero-crossing criterion for fixed-boundary modes has been replaced with a criterion on the zero-crossings of D_C, as defined in Eq. (6). Finally, we have specified an instability criterion for free-boundary modes in Eq. (10), whose value $W_P \equiv P(1)$ is directly computed by the Riccati ODE.

III. SINGULARITIES OF THE SCREW PINCH δW RICCATI ODE

Having presented the equivalent Riccati formulation of Newcomb's screw pinch δW analysis, we now look more closely at some of its details. In particular, we examine the singularities of the cylindrical Riccati ODE defined in Eq. (5). We will see that the singular points of this ODE anticipate salient features of the toroidal Riccati problem to be discussed in Sec. IV.

As before, we note that Eq. (5) shares the same fixed singularities—where $f(r) = 0$—as the Newcomb equation (3). We examine each of these points in turn.

We first consider the behavior of Riccati equation at rational surfaces r_s, where $q(r_s) = m$ and where $f(r_s)$ has a second-order zero. Defining $z \equiv r - r_s$, we expand Eq. (2) near $z = 0$ and find that $f \sim f_2 z^2 + f_3 z^3$ and $g \sim g_0 + g_1 z$ in a generic cylindrical ideal MHD equilibrium with nonzero pressure.[1,3] We substitute a power law ansatz $P \sim A z^\kappa$ into Eq. (5) and find two asymptotic solutions for P at the rational surface, both having $\kappa = 1$

$$P_\pm^{r_s} \sim \alpha_\pm f_2 z. \tag{11}$$

Here, we have defined

$$\alpha_\pm = \frac{-1}{2}\left[1 \pm \sqrt{1 - 4D_S}\right], \quad D_S \equiv -\frac{g_0}{f_2}. \tag{12}$$

As previously referenced, Suydam's criterion[16]

$$D_S < \frac{1}{4} \tag{13}$$

is a necessary condition for the interchange stability of a screw pinch plasma geometry. Although in general this criterion must be checked for satisfaction, we shall assume it to hold and therefore continue our analysis, with coefficients satisfying $\alpha_+ < -1/2$ and $\alpha_- > -1/2$. We refer to $P_+^{r_s}$ of Eq. (11) as the "big" asymptotic solution at r_s and $P_-^{r_s}$ as the "small" asymptotic solution.

One may assess the relative dominance of these asymptotes $P_\pm^{r_s} \sim \alpha_\pm f_2 z$ by substituting a perturbed trajectory $P = P_\pm^{r_s}(r) + \delta P_\pm^{r_s}(r)$ into Eq. (5) and linearizing. We find

$$\delta P_\pm^{r_s\prime}(z) \sim -\frac{2\alpha_\pm}{z}\delta P_\pm^{r_s}(z). \tag{14}$$

Expanding Eq. (12) for small D_S—an especially appropriate ordering for low beta plasmas—suggests $[\alpha_+ \sim -1 + D_S]$ and $[\alpha_- \sim -D_S]$. Therefore, an arbitrarily perturbed solution on approach to r_s will force the Riccati solution to its dominant $P_+^{r_s}$ asymptote, especially for z sufficiently close to 0, as exhibited for $z<0$ on the first plot of Fig. 1.

Solving to next order, we substitute the ansatz $P_\pm^{r_s} \sim \alpha_\pm f_2 z + Cz^\lambda$ into Eq. (5) and keep terms of least order

$$0 \sim \left[C(2\alpha_\pm + \lambda)z^{\lambda-1} - (g_1 + f_3\alpha_\pm^2)z + \frac{C^2}{f_2}z^{2\lambda-2}\right]. \tag{15}$$

Due to the ODE's nonlinearity, the dominant balance of Eq. (15) has solutions with arbitrary coefficient C: The $z^{\lambda-1}$ term vanishes for $\lambda = -2\alpha_\pm$. Of these, the solution $(\lambda = -2\alpha_-) < 1$ is excluded because it would dominate the leading order $\mathcal{O}(z)$ term of $P_-^{r_s}$. However, given $-1 < \alpha_+ < -\frac{1}{2}$ (an ordering typical of low β cylindrical plasmas), the big solution's next leading contribution would appropriately be of order $-2\alpha_+$.

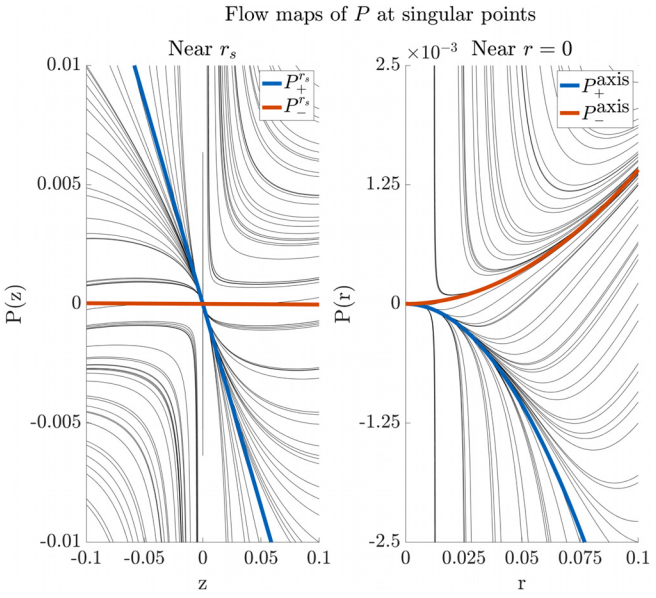

FIG. 1. Asymptotic solutions of the Riccati variable P are plotted near the singularities—the rational surface $(z \equiv r - r_s = 0)$ and magnetic axis $(r = 0)$—of a typical cylindrical equilibrium. The $P_-^{r_s}$ asymptote has a small negative slope, although it may not be apparent.

Additionally, $\lambda = 2$ satisfies dominant balance for the first two terms of Eq. (15), in which case each branch uniquely determines C. We correspondingly distinguish three possible asymptotic solutions to next order

$$\begin{cases} P_+^{r_s} & \sim \alpha_+ f_2 z + \left[\dfrac{g_1 + f_3\alpha_+^2}{2(1+\alpha_+)}\right]z^2, \\ P_+^{r_s}|_{C\neq 0} & \sim \alpha_+ f_2 z + C|z|^{-2\alpha_+}, \\ P_-^{r_s} & \sim \alpha_- f_2 z + \left[\dfrac{g_1 + f_3\alpha_-^2}{2(1+\alpha_-)}\right]z^2. \end{cases} \tag{16}$$

Equation (16) may alternatively be derived by recalling that Riccati solutions are, up to an overall constant, in one-to-one correspondence with solutions of Newcomb's equation—after all, $P = f\xi'/\xi$. Newcomb's Eq. (3) has big and small asymptotic solutions near r_s

$$\xi^{r_s} \sim A\xi_+^{r_s} + B\xi_-^{r_s}, \tag{17}$$

which are readily determined by a Frobenius expansion

$$\xi_\pm^{r_s} = |z|^{\alpha_\pm}\left(1 + \frac{g_1 - f_3\alpha_\pm(2+\alpha_\pm)}{2f_2(1+\alpha_\pm)}z + \cdots\right). \tag{18}$$

[Here, $\alpha_\pm$ is defined as in Eq. (12).] We note that $\xi_\pm^{r_s}/|z|^{\alpha_\pm}$ is analytic near r_s whenever f and g are.[17]

When Eq. (17) is now inserted into Eq. (4), we find again the three expressions of Eq. (16). In particular, when $A=0$ or $B=0$ in Eq. (17), the resulting Riccati asymptotes $P_+^{r_s} \sim f\xi_+^{r_s\prime}/\xi_+^{r_s}$ and $P_-^{r_s} \sim f\xi_-^{r_s\prime}/\xi_-^{r_s}$ are analytic and take the form of the first and last expressions of Eq. (16), respectively. These two solutions are highlighted in the first plot of Fig. 1.

The nonanalytic solution $P_+^{r_s}|_{C\neq 0}$ corresponds to a 'mixed' asymptote ξ^{r_s} for which A and B are nonzero, and the undetermined coefficient C is proportional to B/A. As noted in Eq. (14), any $A \neq 0$ contribution drives P toward its big solution asymptote due to the dominance of $\xi_+^{r_s}$. The mixed solution is C1-continuous, with a generally discontinuous and divergent second derivative. For all solutions, we observe that P and P' are continuous and finite at r_s, with well-defined limits $P(r_s) = 0$ and $P'(r_s) = \alpha_\pm f_2$.

Because of the general non-analyticity of P at r_s, there is some ambiguity about integrating past this singularity. As in treatments of Newcomb's equation, asymptotic solutions must be independently determined on the left and right sides of r_s. In the analysis of this paper, we adopt Newcomb's approach, also used in codes such as PEST2[18] and DCON,[4] which constrain the space of admissible perturbations to those satisfying a finite energy "physicality condition," $\delta W < \infty$. This condition fully determines our treatment of the rational surfaces, as we now describe.

Given the scaling in Eq. (8) of the perturbed potential energy, we can approximate the energy of the big and small asymptotic solutions at the rational surface as follows:

$$\begin{aligned} \delta W_+|_{r_s} &\propto \xi_+^{r_s} P_+^{r_s} \xi_+^{r_s} \propto |z|^{1+2\alpha_+} \sim |z|^{-\sqrt{1-4D_S}} \to \infty \\ \delta W_-|_{r_s} &\propto \xi_-^{r_s} P_-^{r_s} \xi_-^{r_s} \propto |z|^{1+2\alpha_-} \sim |z|^{+\sqrt{1-4D_S}} \to 0. \end{aligned} \tag{19}$$

[Here, we have continued to assume Suydam's criterion, Eq. (13).] Solutions along the big asymptote are seen to have infinite energy at the rational surface.

In Newcomb's analysis, therefore, the $\delta W < \infty$ condition is imposed by using the "small solution crossing" (SSC), which restricts the Newcomb system to its small solution $\xi_-^{r_s}$ at a rational surface. We equivalently restrict the Riccati system to its small asymptote $P_-^{r_s}$. When a rational surface is crossed, the SSC condition requires exiting the singularity along the small $P_-^{r_s}$ asymptote, thereby removing the effect of the asymptotic infinite-energy perturbation $\xi_+^{r_s}$ on the value of δW. We further discuss the constraints that the $\delta W < \infty$ condition places on our Riccati solutions in Sec. VI.

Having determined the asymptotic treatment of Eq. (5) near r_s, we now examine the Riccati ODE's singularity at the magnetic axis, $r = 0$. For ease of presentation, we shall assume that our modes satisfy $|m| > 1$. (Modes $|m| = 0, 1$ require separate treatment.) Accordingly, given asymptotic expansions $f \sim f_3 r^3 + f_4 r^4$ and $g \sim g_1 r + g_2 r^2$ of Eq. (2), typical of cylindrical equilibria[3] for small r, we substitute a power law ansatz $P \sim A r^\kappa$ into Eq. (5) and iterate.

Solving to subleading order, we find

$$P_\pm^{\text{axis}} \sim \eta_\pm f_3 r^2 + \left[\frac{g_2 + f_4 \eta_\pm^2}{3 + 2\eta_\pm}\right] r^3, \tag{20}$$

where

$$\eta_\pm = -\left[1 \pm \sqrt{1 + \frac{g_1}{f_3}}\right]. \tag{21}$$

Expanding Eq. (2), we note that $g_1/f_3 = m^2 - 1$, such that $\eta_\pm = -[1 \pm |m|]$. Therefore, the degree of freedom (DOF) of this first-order nonlinear ODE generally emerges at higher order in the P_+^{axis} expansion—unlike the coefficient C that appeared already in the second term of Eq. (16). In particular, at the axis, a term of the form $P_+^{\text{axis}} \sim \ldots + (D r^{-2\eta_+})$ will eventually appear at higher order in the expansion.

By substituting the ansatz $\xi \sim r^\kappa$ into Eq. (3), it is readily seen that the two asymptotic Riccati solutions $P_\pm^{\text{axis}}$ of Eq. (20) each correspond, respectively, to two asymptotic Newcomb solutions $\xi_\pm^{\text{axis}} \sim r^{\eta_\pm}$. Since $\eta_+ < 0$, however, a regular, $\delta W < \infty$ solution for the perturbation ξ at the magnetic axis requires that we choose $\xi \sim \xi_-^{\text{axis}}$, and therefore $P \sim P_-^{\text{axis}}$, for our Riccati initial condition, as before. In keeping with $\delta W < \infty$, therefore, we initialize the Riccati solution of Eq. (5) by setting $P(\epsilon) = P_-^{\text{axis}}(\epsilon) = f \xi_-^{\prime\text{axis}} / \xi_-^{\text{axis}}|_\epsilon$.

We furthermore note that only the P_-^{axis} asymptote of Eq. (20) is an attractor as we integrate away from $r = 0$. In particular, perturbing our trajectory at the axis as we did in Eq. (14), we find

$$\delta P_\pm^{\text{axis}\prime}(r) \sim -\frac{2\eta_\pm}{r} \delta P_\pm^{\text{axis}}(r). \tag{22}$$

Since $\eta_+ < 0 < \eta_-$ ($\forall\ |m| > 1$), any perturbation to the P_-^{axis} (respectively, P_+^{axis}) is infinitely suppressed (respectively, amplified) for r arbitrarily close to the magnetic axis—as depicted in Fig. 2. As a result, any perturbed solution very near $r = 0$ will converge rapidly to the stable asymptote P_-^{axis} upon exiting from the axis. This observation will be especially relevant in our discussion of the toroidal Riccati system's initial conditions in Sec. IV. We note that this rapid convergence to P_-^{axis} is also visible in the second plot of Fig. 1.

As a final note, we observe that the scalings of $P_\pm^{\text{axis}}$ and $P_\pm^{r_s}$ in Eqs. (16) and (20), respectively, render P finite—zero, in fact—at all of the Riccati ODE's fixed singularities. This quiescent behavior contrasts

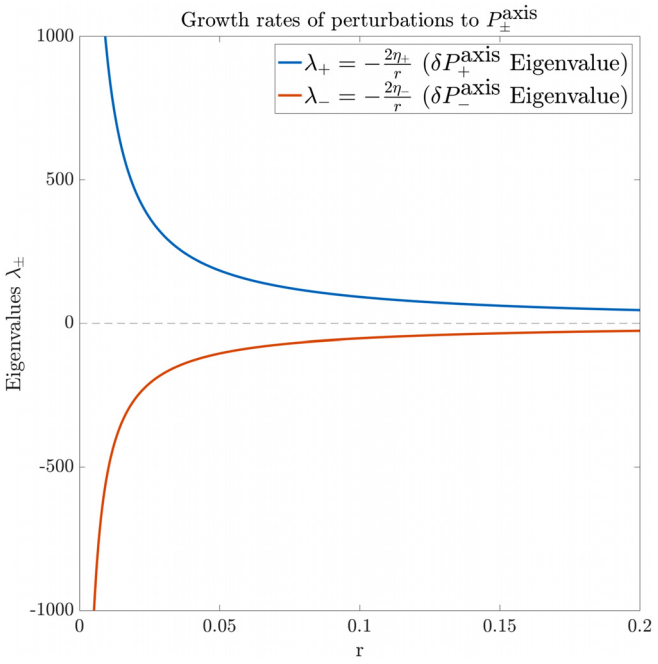

FIG. 2. The above plot depicts the growth rates of perturbations to the two asymptotic solutions $P_\pm^{\text{axis}}$ near $r = 0$, as defined in Eq. (22). As P is integrated away from the axis, P_-^{axis} behaves as an attractor solution.

with the divergence of the corresponding Newcomb solutions. We note, however, that while the preceding analysis has established this behavior of P at the fixed singularities of Eq. (5), we have not specified a numerical treatment for the nonlinear ODE's spontaneous singularities,[19] where P diverges and $D_C \to 0$. Clearly, such points cannot be integrated over without some numerical strategy.

The spontaneous singularities of the Riccati equation are a well-known and commonly addressed feature of Riccati systems. For now, we simply observe that the ODE for $R \equiv 1/P$—which passes through zero at the spontaneous singularities of P—may be integrated instead

$$R' = -\frac{P'}{P^2} = \frac{1}{f} - gR^2. \tag{23}$$

[R is the very same critical determinant of Eq. (6).] We delay a detailed discussion of the "complementary" Riccati ODE of Eq. (23) until Sec. IV, where spontaneous singularities of the toroidal Riccati equation are addressed in an entirely analogous manner.

IV. THE δW RICCATI APPROACH FOR AXISYMMETRIC TOROIDAL EQUILIBRIA

We now study the δW Riccati formulation for axisymmetric toroidal plasmas. Referring the reader to Refs. 4 and 5 for greater detail, we begin by recalling that toroidal perturbations may be Fourier-decomposed into sums of normal modes of the form

$$\xi_{m,n}(\mathbf{x}) = \xi_{m,n}(\psi) e^{i(m\theta - n\zeta)}. \tag{24}$$

Here, (ψ, θ, ζ) represent the flux function (radial), poloidal, and toroidal coordinates and (m, n) are the poloidal and toroidal mode

numbers, respectively, of the plasma displacement ξ. Since modes couple along the poloidal mode number and decouple along toroidal mode number in tokamak geometries, we can take n to be single-valued and index the coupled poloidal Fourier modes by a set of cardinality $\#\{m\} = M$.

We describe an arbitrary perturbation by the variable $\boldsymbol{\Xi}(\psi)$, which denotes an $M \times 1$ vector of Fourier mode amplitudes $\xi_{m,n}(\psi)$. A Lagrangian for the change in plasma potential energy due to $\boldsymbol{\Xi}$ is then defined by[4]

$$\delta W = \int_0^1 L(\boldsymbol{\Xi}, \boldsymbol{\Xi}', \boldsymbol{\Xi}^\dagger, \boldsymbol{\Xi}^{\dagger\prime}) \mathrm{d}\psi = \frac{1}{2}\int_0^1 \left(\boldsymbol{\Xi}^{\dagger\prime}\mathbf{F}\boldsymbol{\Xi}' + \boldsymbol{\Xi}^{\dagger\prime}\mathbf{K}\boldsymbol{\Xi} + \boldsymbol{\Xi}^\dagger\mathbf{K}^\dagger\boldsymbol{\Xi}' + \boldsymbol{\Xi}^\dagger\mathbf{G}\boldsymbol{\Xi}\right)\mathrm{d}\psi, \tag{25}$$

where $' \equiv d/d\psi$ and † denotes a conjugate transpose. Here, the matrices $\{\mathbf{F} = \mathbf{F}^\dagger, \mathbf{G} = \mathbf{G}^\dagger, \mathbf{K}\} \in \mathbb{C}^{M\times M}$ encode data about the plasma equilibrium and geometry.

The toroidal Newcomb equation may be derived as the Euler–Lagrange equation of this Lagrangian

$$-(\mathbf{F}\boldsymbol{\Xi}' + \mathbf{K}\boldsymbol{\Xi})' + (\mathbf{K}^\dagger\boldsymbol{\Xi}' + \mathbf{G}\boldsymbol{\Xi}) = 0, \tag{26}$$

or, written in its Hamiltonian form

$$\begin{pmatrix}\mathbf{q}\\ \mathbf{p}\end{pmatrix}' = \begin{pmatrix}-\mathbf{F}^{-1}\mathbf{K} & \mathbf{F}^{-1}\\ \mathbf{G} - \mathbf{K}^\dagger\mathbf{F}^{-1}\mathbf{K} & \mathbf{K}^\dagger\mathbf{F}^{-1}\end{pmatrix}\begin{pmatrix}\mathbf{q}\\ \mathbf{p}\end{pmatrix}. \tag{27}$$

The canonical coordinates $(\mathbf{q}, \mathbf{p}^\dagger) = (\boldsymbol{\Xi}, [\mathbf{F}\boldsymbol{\Xi}' + \mathbf{K}\boldsymbol{\Xi}]^\dagger)$ denote the Fourier-decomposed perturbations $\boldsymbol{\Xi}$ and their conjugate momenta—as in Eq. (4). The coordinate ψ is used as an effective time coordinate in this Hamiltonian system.

The Riccati transformation of Eq. (27) proceeds analogously to the cylindrical case, by defining an $M \times M$ linear transformation $\mathbf{P}$ such that

$$\mathbf{p}(\psi) = \mathbf{P}(\psi)\mathbf{q}(\psi). \tag{28}$$

Plugging this transformation into Eq. (27) yields the matrix Riccati differential equation (MRDE) for $\mathbf{P}$

$$\mathbf{P}' = \mathbf{G} - [\mathbf{P} - \mathbf{K}^\dagger]\mathbf{F}^{-1}[\mathbf{P} - \mathbf{K}]. \tag{29}$$

It is seen that $\mathbf{P}$ is Hermitian when initialized as such. We note that whereas the MRDE of Eq. (29) solves for the $M \times M$ Riccati matrix, the full basis of linearly independent solutions to Eq. (27) in general comprises a $2M \times 2M$ matrix.

Equation (28) suggests an important relationship between the solutions of Eqs. (27) and (29). Given a $2M \times M$ matrix of modes $\mathbf{U}(\psi) \equiv \begin{bmatrix}\mathbf{Q}(\psi)\\ \mathbf{P}(\psi)\end{bmatrix}$ that satisfy the Hamiltonian equation (27), the associated Riccati matrix is fully specified by

$$\mathbf{P} = \mathbf{P}\mathbf{Q}^{-1}, \tag{30}$$

as in Eq. (4). (We call attention to the serif and sans-serif fonts in this expression.) We note that linear combinations of the columns of $\mathbf{U}$—i.e., $\mathbf{U}\cdot\mathbf{C} = \begin{bmatrix}\mathbf{Q}\cdot\mathbf{C}\\ \mathbf{P}\cdot\mathbf{C}\end{bmatrix}$ for some invertible constant matrix $\mathbf{C} \in \mathbb{C}^{M\times M}$—leave $\mathbf{P}$ invariant. In this sense, the Riccati approach removes extraneous degrees of freedom, which turn out to be irrelevant to a δW stability analysis.

The Newcomb procedure for the toroidal δW problem was first defined in Ref. 4. We reframe the procedure in the Riccati formulation as follows: (i) Mercier's criterion[20] (to be defined) for interchange stability is checked; (ii) assuming that Mercier's criterion is satisfied, Eq. (29) is integrated from the magnetic axis ($\psi = 0$) to the plasma edge ($\psi = 1$) with small initial conditions (to be defined); (iii) after each rational surface $0 < \psi_s < 1$—where the ODE is singular—$\mathbf{P}$ is re-initialized again with a small solution and integrated forward; (iv) if the resulting integrated solution has any conjugate points—that is, if $\mathbf{P}$ has any infinities—then, the plasma is unstable to fixed-boundary modes; otherwise, it is stable to such modes.

The "infinities" of the Riccati ODE define an instability criterion for fixed-boundary perturbations in the toroidal system

$$\mathbf{D}_C \equiv \mathbf{det}[\mathbf{P}^{-1}] = 0, \tag{31}$$

where $\mathbf{P}$ is the solution to Eq. (29). This criterion, discovered in Ref. 4, mirrors Eq. (6) for the cylindrical case. A toroidal equilibrium is stable to fixed-boundary modes if the critical determinant $\mathbf{D}_C$ is non-vanishing for all $\psi \in (0, 1)$.

Having defined a toroidal stability criterion for fixed-boundary modes, we now examine the stability of free-boundary modes. Following the argument of Eqs. (7) and (8), we define, differentiate, and integrate a function $S(\psi)$ to find

$$S(\psi) \equiv \frac{1}{2}\boldsymbol{\Xi}^\dagger(\psi)\mathbf{P}(\psi)\boldsymbol{\Xi}(\psi) = \int_0^\psi L(\boldsymbol{\Xi}, \boldsymbol{\Xi}', \boldsymbol{\Xi}^\dagger, \boldsymbol{\Xi}^{\dagger\prime})\mathrm{d}\tilde{\psi}, \tag{32}$$

where we have required $S(0) = 0$. Once again, $\mathbf{P}(\psi)$ is a Hermitian bilinear form that maps a perturbation $\boldsymbol{\Xi}(\psi)$ to its cumulative extremal energetic cost over $[0, \psi]$.

As in the cylindrical case, Eq. (32) suggests a free-boundary stability criterion as well. In particular, if a plasma is both Mercier- and fixed-boundary-stable, then the solutions $\boldsymbol{\Xi}(\psi)$ of Eq. (26) are not only extremal but minimize δW. Accordingly, the Riccati solution $\mathbf{P}(1)$ maps an edge perturbation to its minimal energy

$$S(1) = \frac{1}{2}\boldsymbol{\Xi}^\dagger(1)\mathbf{P}(1)\boldsymbol{\Xi}(1). \tag{33}$$

We therefore define the toroidal plasma response matrix, $\mathbf{W}_P \equiv \mathbf{P}(1)$.

As described in Ref. 4, we must further incorporate the perturbed energy of the magnetized vacuum around the plasma, whose energetic contribution can be described by $\frac{1}{2}\boldsymbol{\Xi}^\dagger(1)\mathbf{W}_V\boldsymbol{\Xi}(1)$. The vacuum response matrix $\mathbf{W}_V$ may be calculated independently of $\mathbf{W}_P$, as with the VACUUM code.[21,22] For a Mercier- and fixed-boundary-stable toroidal plasma, therefore, the total bilinear form $\mathbf{W}_T \equiv \mathbf{W}_P + \mathbf{W}_V$ maps an arbitrary perturbation $\boldsymbol{\Xi}(1)$ to its minimal energetic effect on the full system.

The eigenvalues of this bilinear form correspondingly define an instability criterion

$$\min_i \boldsymbol{\lambda}_i[\mathbf{W}_P + \mathbf{W}_V] < 0, \tag{34}$$

where $\boldsymbol{\lambda}_i[\cdot]$ represents the ith matrix eigenvalue. That is, a toroidal equilibrium is unstable to free-boundary modes if any eigenvalue of

the total response matrix $\mathbf{W}_T$ is negative. This criterion is a straightforward generalization of Eq. (10).

While the broad structure of the toroidal δW Riccati problem largely follows its cylindrical counterpart, it remains for us to examine the numerical details of the toroidal solution. In particular, we now describe our strategy for integrating Eq. (29) near its singular points.

We first consider the initial condition of the toroidal Riccati ODE at the magnetic axis. We recall that in Refs. 4 and 5, the small initial conditions $\mathbf{q}(0) = 0$ were approximately imposed for the toroidal Newcomb system of Eq. (27) by setting

$$\left.\begin{bmatrix}\mathbf{Q}\\ \mathbf{P}\end{bmatrix}\right|_{\psi=\epsilon} = \begin{bmatrix}\mathbb{0}_M\\ \mathbb{1}_M\end{bmatrix}. \tag{35}$$

As in Eq. (30), here $\mathbf{Q}$ and $\mathbf{P}$ denote $M \times M$ fundamental matrices of solutions to Eq. (27), while $\mathbb{0}_M$ and $\mathbb{1}_M$ denote the $M \times M$ null and identity matrices, respectively. $0 < \epsilon \ll 1$ describes a small distance from the singular point at the magnetic axis, $\psi = 0$. Initializing toroidal modes slightly off-axis yields solutions across the plasma region, which are consistent with the asymptotically regular solutions at $\psi = 0$.[3,4] This consistency is the result of the rapid convergence toward an attractor solution, as described in Eq. (22), and depicted in the second plot of Fig. 1 for the analogous cylindrical system.

To implement the corresponding initial conditions for our toroidal Riccati system, we plug Eq. (35) into Eq. (30). We find that the initial condition of Eq. (35) corresponds to a divergent Riccati matrix $\mathbf{P}(\epsilon) \to \infty$. This seemingly ill-defined initial condition is readily implemented by employing the complementary matrix Riccati differential equation[23] (CMRDE) for the inverse of the plasma response matrix, $\mathbf{R} \equiv \mathbf{P}^{-1}$

$$\begin{aligned}\mathbf{R}' = (\mathbf{P}^{-1})' &= -\mathbf{P}^{-1}\mathbf{P}'\mathbf{P}^{-1}\\ &= -\mathbf{RGR} + [\mathbb{1} - \mathbf{RK}^\dagger]\mathbf{F}^{-1}[\mathbb{1} - \mathbf{KR}].\end{aligned} \tag{36}$$

Clearly, the corresponding initial condition for the CMRDE should be $\mathbf{R} = \mathbb{0}_M$. In practice, therefore, we integrate our Riccati solution by initializing Eq. (36) with $\mathbf{R}|_{\psi=\epsilon} = \mathbb{0}_M$.

Although the CMRDE of Eq. (36) was defined to help initialize the Riccati ODE, it serves an important and more general role in our solution of the δW Riccati problem. In particular, when the magnitude of $\mathbf{R}(\psi)$ grows sufficiently large after its integration away from the magnetic axis, we invert it and continue integrating $\mathbf{P}$ via Eq. (29). Thereafter, when $\mathbf{P}$ grows beyond some bound, we invert again and integrate $\mathbf{R}$ from that point. We may continue in this way until the plasma edge is reached, constraining the growth of our Riccati solution by "bouncing" between integrations of Eqs. (29) and (36) until $\mathbf{P}(1)$ is found.

Indeed, because nonlinear ODEs can exhibit spontaneous singularities—just as we noted in our discussion near Eq. (23) for $R \equiv P^{-1}$—such a technique is sometimes necessary to solve for $\mathbf{P}(1)$. The spontaneous singularities of Riccati equations are a common and readily solvable feature of Riccati systems and have been addressed in the literature by several methods, including CMRDEs and Möbius schemes.[23,24] We note that this method of bouncing between integrating R and P can be equally well applied in the cylindrical case, using Eqs. (5) and (23).

Having described our strategies for integration away from $\psi = 0$ and through spontaneous singularities, we now examine Eq. (29) near rational surfaces ψ_s, where $q(\psi_s) = m/n$. As in the cylindrical case, we will find that the Riccati ODE avoids the divergent solutions of its linear counterpart Eq. (27) at such points.

We first recall a decomposition of the $\{\mathbf{F}, \mathbf{G}, \mathbf{K}\}$ matrices described in Ref. 4

$$\mathbf{F} = \mathbf{Q}\bar{\mathbf{F}}\mathbf{Q}, \quad \mathbf{K} = \mathbf{Q}\bar{\mathbf{K}}, \quad \mathbf{G} = \bar{\mathbf{G}}, \tag{37}$$

where $\bar{\mathbf{F}}$, $\bar{\mathbf{G}}$, and $\bar{\mathbf{K}}$ are nonsingular $\mathbb{C}^{M\times M}$ matrices and where

$$\mathbf{Q}_{m,m'} \equiv [m - nq(\psi)]\delta_{m,m'}. \tag{38}$$

In Eq. (38), exactly one diagonal element of $\mathbf{Q}$ is seen to vanish at each rational surface ψ_s. We define $z \equiv \psi - \psi_s$ and note that the singular row of $\mathbf{K}$ and row and column of $\mathbf{F}$ scale as z near $z = 0$, while the doubly singular diagonal element of $\mathbf{F}$ scales as z^2. Observing that $\mathbf{Q}_{mm} \sim -nq'(\psi_s)z$ near ψ_s, we substitute Eq. (37) into Eq. (29) to find linearly vanishing asymptotes for the singular row and column of $\mathbf{P}$ as $\psi \to \psi_s$

$$\mathbf{P}_{im}(z), \mathbf{P}_{mi}(z) \propto z, \quad \text{as } z \to 0 \ \forall\, i. \tag{39}$$

The C1-continuity of $\mathbf{P}$ at $z = 0$ contrasts with the solutions of the Newcomb Eq. (27), which diverge at toroidal rational surfaces most stiffly in high β and low q' shear plasmas.

As in the cylindrical case, the toroidal Riccati equation has big and small resonant asymptotes at ψ_s, corresponding to the big and small solutions of Eq. (27). To satisfy the $\delta W < \infty$ condition and cross ψ_s via SSC, we must similarly constrain these resonant solutions for $\mathbf{P}$ to the small asymptote.

One strategy to compute the asymptotic solutions of Eq. (27) would be to follow the Frobenius method of Turrittin[25] introduced in Ref. 4. This method generates $2M \times 2M$ matrices $\mathbf{U}(\psi_s \pm \epsilon)$, whose columns form complete bases for asymptotic solutions of Eq. (27) on the left and right sides of ψ_s, respectively. Each matrix $\mathbf{U}_{\pm\epsilon}$ has two singular columns with leading order behavior $\propto |z|^{\tilde{\alpha}_\pm}$, where $\tilde{\alpha}_\pm \equiv \pm\sqrt{-D_I}$. Here, D_I is the Mercier parameter for axisymmetric toroidal interchange stability.[4,20] Although Turrittin's method is not directly applicable to the nonlinear Riccati equation, the resonant modes of $\mathbf{U}_{\pm\epsilon}$ could in principle be used to identify the resonant asymptotes of $\mathbf{P}$ at ψ_s, via Eq. (30).

However, we instead find that a straightforward numerical approximation imposes the desired SSC constraint to high accuracy. In particular, to cross ψ_s via SSC, we leverage the dominance of the big solution on approach to ψ_s, and the dominance of the small solution upon exiting ψ_s. In particular, we identify the singular eigenvector $\mathbf{v}_0$ of $\mathbf{P}_{-\epsilon} \equiv \mathbf{P}(\psi_s - \epsilon)$, whose eigenvalue approaches 0 at ψ_s along the big solution asymptote, and project it out

$$\mathbf{P}_{+\epsilon} = \left(\mathbb{1} - \mathbf{v}_0\mathbf{v}_0^\dagger\right)\mathbf{P}_{-\epsilon}. \tag{40}$$

Since the small solution is an attractor solution when integrating away from the singularity, it then dominates the resonant subspace as $\mathbf{P}$ is integrated away from ψ_s. We note that, in addition to the resonant eigenvalue passing linearly through 0, the matrix $\mathbf{P}$ also has $M - 1$ nonvanishing eigenvalues at ψ_s, which pass continuously through ψ_s and are unaffected by Eq. (40). As we shall see in Sec. V, this implementation of SSC for the Riccati system accurately reproduces the results of DCON's δW analysis.

We have thus specified our treatment of $\mathbf{P}$ at its fixed singularities $\{\psi = 0, \psi_s\}$ and spontaneous singularities $\{\psi|_{\mathbf{D}_C(\psi)=0}\}$. For

completeness, we note that the plasma separatrix (if it exists) is also a fixed singularity of the toroidal Riccati ODE, at $\psi = 1$. However, as suggested in Ref. 4, our integration is simply truncated at $\psi = 1 - \epsilon_{\text{edge}}$ for some small ϵ_{edge} to avoid the plasma edge.

V. NUMERICAL RESULTS

Having detailed our approach the toroidal Riccati δW problem, we now discuss its numerical performance. We first describe the significantly improved numerical behavior of the Riccati solution near the magnetic axis. The M stiff solutions of Eq. (27) quickly span $\mathcal{O}(M) \sim 40$ orders of magnitude for typical tokamak equilibria when integrated away from the magnetic axis. On the other hand, we find that our bouncing technique for the Riccati system—which switches between integrations of $\mathbf{P}$ and $\mathbf{R}$ (as described in Sec. IV)—successfully bounds its solutions for such equilibria. The norms of $\mathbf{P}$ and $\mathbf{R}$ are constrained throughout their integration, with $\|\mathbf{P}\|_\infty, \|\mathbf{R}\|_\infty \lesssim 10^6$. This feature could be decisive in δW analyses for high-resolution toroidal plasma equilibria that may require hundreds of modes to achieve a convergent result at the plasma core.

This improved performance can be simply explained by appealing to the cylindrical Riccati equation. We recall that the condition number of a differentiable function $f(x)$ is defined by

$$\mathbf{cond}(f(x)) = \left| \frac{xf'(x)}{f(x)} \right|. \tag{41}$$

In our discussion following Eq. (21), we noted that the regular cylindrical perturbations ξ behave as $\xi_-^{\text{axis}} \sim r^{\eta_-}$ at the axis. The Newcomb solution therefore has $\mathbf{cond}(\xi_-^{\text{axis}}(r)) \sim \eta_-$. On the other hand, $P_-^{\text{axis}} \sim \eta_- f_3 r^2$ has condition number $\mathbf{cond}(P_-^{\text{axis}}(r)) \sim 2$ near the magnetic axis. Since $\eta_- = |m| - 1$ grows with poloidal mode number m, the Newcomb ODE for cylindrical perturbations becomes increasingly ill-conditioned for higher m modes, whereas the condition number of Riccati solutions is unaffected. For toroidal equilibria, in which tens or hundreds of modes might be present, this mode-invariant scaling of the Riccati solution can be a helpful asset.

We benchmark the accuracy of the Riccati ODE by comparing the eigenvalues of $\mathbf{P}(1)$ with DCON. Integrating Eq. (29) with the complex adaptive integrator ZVODE,[27] we implement the various aspects of our toroidal Riccati procedure, including the initialization $\mathbf{R} = \mathbb{0}_M$ of Eq. (36) at $\psi = \epsilon$ and the SSC crossing method of Eq. (40). The eigenvalues of the resulting plasma response matrix $\mathbf{P}(1)$ achieve a highly accurate reproduction of the δW analysis of DCON, as depicted in Fig. 3. We have thus successfully benchmarked our Riccati integration.

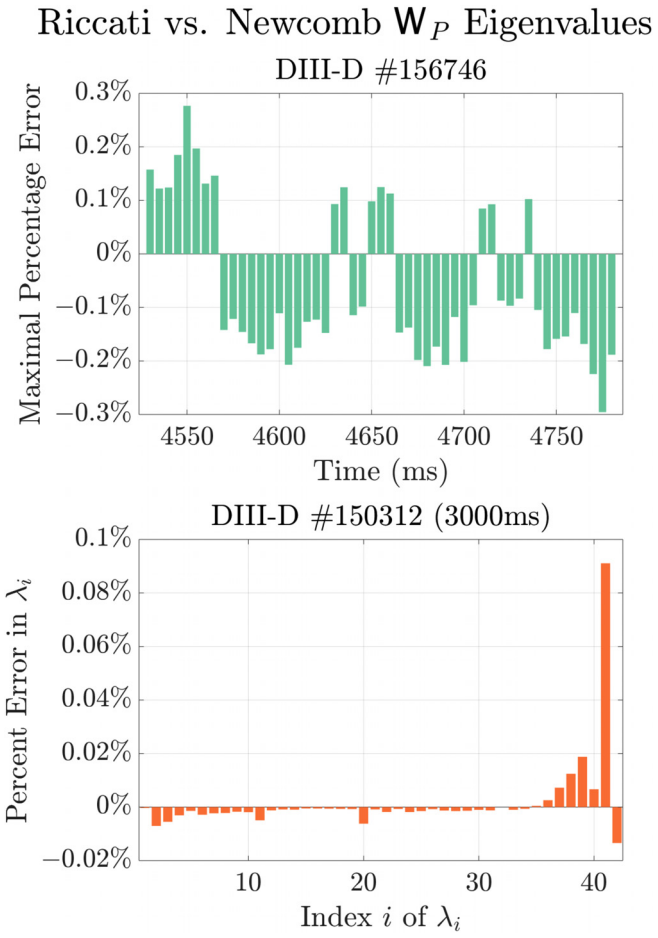

FIG. 3. These charts benchmark the eigenvalues of the toroidal plasma response matrix $\mathbf{W}_P \equiv \mathbf{P}(1)$, as calculated by the Riccati ODE against the output of DCON.[4] Top: This chart displays the worst percentage error in any single eigenvalue of $\mathbf{W}_P$ for equilibrium fitting (EFIT)[26] reconstructions of several time slices of DIII-D shot #156764. Bottom: This chart depicts the percentage error measured for each of the 42 ordered eigenvalues $\lambda_1 > \cdots > \lambda_{42}$ of $\mathbf{W}_P$, for a hand-fit reconstruction of the 3000 ms time slice of DIII-D shot #150312. The least eigenvalue, λ_{42}, corresponds to the minimal-energy plasma response.

VI. DISCUSSION: THE MINIMIZATION OF δW BY ADMISSIBLE PERTURBATIONS

As a final point of discussion, we now consider the effect of the admissibility criterion $\delta W(\xi^*, \xi) < \infty$ on the behavior of extremal perturbations. In a cylindrical geometry, $\delta W < \infty$ limits us to solutions that are small—P_- and ξ_-—at both the magnetic axis $r = 0$ and rational surfaces r_s. As demonstrated in Fig. 4, however, a solution of Eqs. (3) or (5) that is small at a given singularity almost always maps to the big solution at other singularities (except in marginal cases). As a result, the only admissible extremal solution of Eq. (3) on the interval $[0, r_s]$ that is small at both endpoints is the degenerate solution $0 = [\xi;\ \xi']_{0 \le r \le r_s}$. (We note that $P = f\xi'/\xi$ is not well-defined for such solutions.)

On the other hand, the free-boundary mode on the remaining interval $[r_s, 1]$ has only one small boundary condition to satisfy at r_s. For a cylindrical geometry with one singular surface, therefore, free-boundary stability only requires integrating $P_-^{r_s}$ (or $\xi_-^{r_s}$) on the subinterval $[r_s, 1]$. (See also Ref. 1.) It is worth noting that if we put a conducting wall—as Newcomb does[3]—at the plasma edge $r = 1$, then the only admissible solution on $[r_s, 1]$ would again be the degenerate one, $\xi = 0$. It is only the relaxation of this condition, by putting a vacuum region at the edge of the plasma, which allows for nonzero extremal free-boundary modes.

It is natural to wonder if the over-determined small boundary conditions in the plasma core could alternatively be accommodated by allowing perturbations to take the form of "broken" extremals.

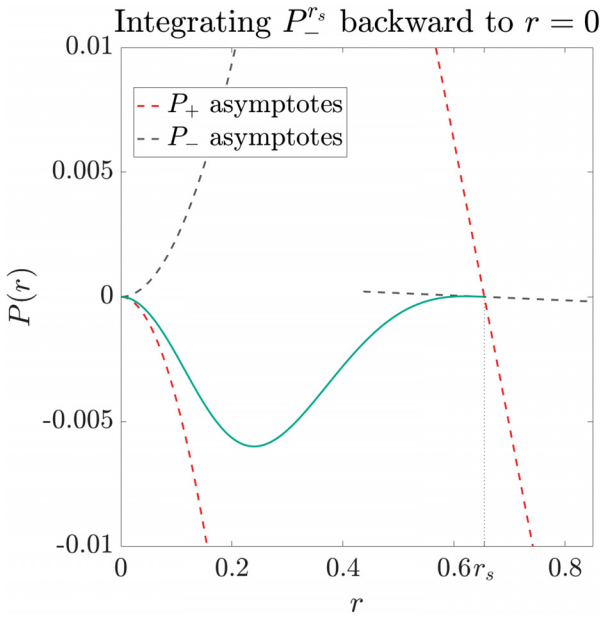

FIG. 4. This plot demonstrates that a solution of Eq. (5), initialized on the small asymptote $P_-^{r_s}$ at r_s, coincides with the big solution asymptote P_+^{axis} when integrated backward to the magnetic axis.

In Eq. (3), for example, one might attempt to find a nonsingular point $0 < r_* < r_s$ at which ξ_-^{axis} on $[0, r_*]$ could be continuously joined to $\xi_-^{r_s}$ on $[r_*, r_s]$ (with a 'break' formed by their discontinuous derivative).

However, the Weierstrass–Erdmann (W − E) condition[13] asserts that it is never energetically advantageous to break the extremals of the quadratic Lagrangian in Eq. (1) at nonsingular points. In particular, when attempting to join two extremals ξ_1 and ξ_2 at a nonsingular point r_*, W − E requires the jump condition

$$0 = \left[\frac{\partial L}{\partial \xi'}\right]_{r_*-\epsilon}^{r_*+\epsilon} \overset{\text{Eq. (1)}}{\Longrightarrow} f\xi_1'|_{r_*-\epsilon} = f\xi_2'|_{r_*+\epsilon}, \tag{42}$$

as $\epsilon \to 0$. W − E therefore requires that both ξ and ξ' are continuous at any point where $f(r) \neq 0$—i.e., that $\xi_1 = \xi_2$. Indeed, no broken extremal satisfying $\delta W < \infty$ will minimize δW more than the degenerate Euler–Lagrange solution $\xi = 0$ on $[0, r_s]$.

An analogous constraint occurs in toroidal geometries with several rational surfaces $\{\psi_s^i\}_{i=1}^N$. To construct global solutions of Eq. (27) that satisfy $\delta W < \infty$, the "big solution subspaces" $\mathbf{u}_{\text{big}}^{j\pm}(\psi_s^{j\pm}) \equiv \begin{bmatrix}\mathbf{q}\\ \mathbf{p}\end{bmatrix}_{\text{big}}(\psi_s^{j\pm})$ must be zeroed on the left and right sides of each rational surface $\psi_s^{j\pm} \equiv (\psi_s^j \pm \epsilon)$, and $\mathbf{u}_{\text{big}}^{0+}(\epsilon)$ must be zeroed at the magnetic axis. This restriction generally results in the removal of $N+1$ independent solutions at the magnetic axis, where N is the number of singular surfaces. This loss of dimensionality in the solution space is recovered at the plasma edge, however—as it is in the cylindrical case—by the reinstatement of the small solution at each rational surface. At a given surface ψ_s^{i+}, we note that only the component of the small solution $\mathbf{u}_{\text{small}}^{i+}$ that is orthogonal to big solutions mapped back to ψ_s^{i+}—that is

$$\left[\mathbf{u}_{\text{small}}^{i+} - \sum_{j>i} \mathbf{u}_{\text{big}}^{j-} \frac{\langle \mathbf{u}_{\text{small}}^{i+}, \mathbf{u}_{\text{big}}^{j-}\rangle}{\langle \mathbf{u}_{\text{big}}^{j-}, \mathbf{u}_{\text{big}}^{j-}\rangle}\right]_{\psi=\psi_s^{i+}}, \tag{43}$$

should be reinstated. This procedure is carried out near singular surfaces in the DCON code, simply by integrating from the axis to the edge and eliminating the big solution on approach to each singular surface.[4] The corresponding Riccati procedure is defined in Eq. (40).

VII. SUMMARY AND CONCLUSION

We have demonstrated that the Riccati ODE of Eq. (29) offers a practical alternative to the Newcomb equation for the calculation of δW stability, and we identified several techniques for its solution. We have described both the accuracy and improved numerical performance of the Riccati ODE—especially at the magnetic axis. While a nonlinear Riccati δW analysis is slower to evaluate than its (parallelizable) linear counterpart, its numerical performance may enable the δW analysis of otherwise intractable plasma equilibria that require high resolution and many modes to describe. This numerical outperformance was shown to be particularly beneficial at the magnetic axis of toroidal equilibria, where Riccati solutions are substantially better conditioned. We have also brought dynamical system insights into our study of the Riccati equation's behavior at singular points.

Analytically, the Riccati approach is a more direct solution to the δW stability problem; the eigenvalues of the toroidal Riccati matrix characterize fixed- and free-boundary ideal MHD stability—as in Eqs. (31) and (34). Rather than finding the perturbed modes that minimize δW via Eq. (27), whose particular linear combinations are irrelevant to a δW stability analysis, the Riccati method solves for the stability characteristics of the system directly. In this way, it further sharpens our understanding of Newcomb's stability criterion.

ACKNOWLEDGMENTS

The authors thank Amlan Sinha for helpful discussions and our reviewers for their enlightening comments. This research was supported in part by the United States Department of Energy (DoE) under Contract Nos. DE-FC02-04ER54698 and DE-AC02-09CH11466 and the DoE Early Career Research Program: DE-SC0015878.

REFERENCES

[1] J. P. Freidberg, *Ideal MHD* (Cambridge University Press, Cambridge, 2014).
[2] I. Bernstein, E. Frieman, M. Kruskal, and R. Kulsrud, "An energy principle for hydromagnetic stability problems," Proc. R. Soc. London. Ser. A **244**, 17–40 (1958).
[3] W. A. Newcomb, "Hydromagnetic stability of a diffuse linear pinch," Ann. Phys. **10**, 232–267 (1960).
[4] A. H. Glasser, "The direct criterion of Newcomb for the ideal MHD stability of an axisymmetric toroidal plasma," Phys. Plasmas **23**, 072505 (2016).
[5] A. S. Glasser, E. Kolemen, and A. H. Glasser, "A Riccati solution for the ideal MHD plasma response with applications to real-time stability control," Phys. Plasmas **25**, 032507 (2018).
[6] D. G. Luenberger, *Introduction to Dynamic Systems* (John Wiley & Sons, Inc., New York, 1979).
[7] R. M. Murray, *Optimization-Based Control* (California Institute of Technology, CA, 2010).
[8] B. D. O. Anderson and J. B. Moore, *Linear Optimal Control* (Prentice-Hall, Inc., Englewood Cliffs, NJ, USA, 1971).
[9] E. Davison and M. Maki, "The numerical solution of the matrix Riccati differential equation," IEEE Trans. Autom. Control **18**, 71–73 (1973).

[10]C. Kenney and R. Leipnik, "Numerical integration of the differential matrix Riccati equation," IEEE Trans. Autom. Control **30**, 962–970 (1985).
[11]A. S. Glasser and E. Kolemen, "A robust solution for the resistive MHD toroidal Δ' matrix in near real-time," Phys. Plasmas **25**, 082502 (2018).
[12]C. H. Choi and A. J. Laub, "Efficient matrix-valued algorithms for solving stiff Riccati differential equations," IEEE Trans. Autom. Control **35**, 770–776 (1990).
[13]I. Gelfand and S. Fomin, *Calculus of Variations* (Prentice-Hall, Inc., Englewood Cliffs, NJ, 1963).
[14]R. W. Brockett, *Finite Dimensional Linear Systems* (John Wiley and Sons, Inc., New York, 1970).
[15]D. Liberzon, *Calculus of Variations and Optimal Control Theory* (Princeton University Press, Princeton, NJ, 2012).
[16]R. Suydam, "Stability of a linear pinch," in *Proceedings of the Second International Conference on the Peaceful Uses of Atomic Energy* (United Nations, Geneva, 1958), Vol. 31, p. 157.
[17]E. A. Coddington, *An Introduction to Ordinary Differential Equations* (Dover Publications, Inc., New York, 1961).
[18]R. C. Grimm, R. L. Dewar, and J. Manickam, "Ideal MHD stability calculations in axisymmetric toroidal coordinate systems," J. Comput. Phys. **49**, 94–117 (1983).
[19]C. M. Bender and S. A. Orszag, *Advanced Mathematical Methods for Scientists and Engineers I* (Springer New York, New York, NY, 1999).
[20]C. Mercier, "Un critère necéssaire de stabilité hydromagnetique pour un plasma en symétrie de révolution," Nucl. Fusion **1**, 47 (1960).
[21]M. S. Chance, "Vacuum calculations in azimuthally symmetric geometry," Phys. Plasmas **4**, 2161–2180 (1997).
[22]M. Chance, A. Turnbull, and P. Snyder, "Calculation of the vacuum Green's function valid even for high toroidal mode numbers in tokamaks," J. Comput. Phys. **221**, 330–348 (2007).
[23]C. K. Garrett, "Numerical integration of matrix Riccati differential equations with solution singularities," Ph.D. thesis (The University of Texas at Arlington, 2013).
[24]J. Schiff and S. Shnider, "A natural approach to the numerical integration of Riccati differential equations," SIAM J. Numer. Anal. **36**, 1392–1413 (1999).
[25]H. L. Turrittin, "Convergent solutions of ordinary linear homogeneous differential equations in the neighborhood of an irregular singular point," Acta Math. **93**, 27–66 (1955).
[26]L. L. Lao, H. S. John, R. D. Stambaugh, A. G. Kellman, and W. Pfeiffer, "Reconstruction of current profile parameters and plasma shapes in tokamaks," Nucl. Fusion **25**, 1611 (1985).
[27]A. C. Hindmarsh, "ODEPACK, a systematized collection of ODE solvers," in *Scientific Computing*, edited by R. Stepleman (North-Holland, Amsterdam, 1983).